MECHANICAL PROPERTY CHARACTERIZATION OF MULTIDIRECTIONAL Si_3N_4/BN FIBROUS MONOLITHS*

M. Tlustochowicz, D. Singh, W. A. Ellingson, and K. C. Goretta
Energy Technology Division
Argonne National Laboratory
Argonne, IL 60439

M. Rigali and M. Sutaria
Advanced Ceramics Research, Inc.
Tucson, AZ 85713

June 1999

Proc. 101st Annual Meeting of the American Ceramic Society, Indianapolis, April 25-28 1999.

*Work supported by the Defense Advanced Research Projects Agency through a U.S. Department of Energy Interagency Agreement, under Contract W-31-109-Eng-38.

DISCLAIMER

Portions of this document may be illegible in electronic image products. Images are produced from the best available original document.

MECHANICAL PROPERTY CHARACTERIZATION OF MULTIDIRECTIONAL Si_3N_4/BN FIBROUS MONOLITHS

M. Tlustochowicz, D. Singh, W. A. Ellingson, and K. C. Goretta
Energy Technology Division
Argonne National Laboratory, Argonne, IL 60439

M. Rigali and M. Sutaria
Advanced Ceramics Research, Inc.
Tucson, AZ 85713

ABSTRACT

Fibrous monoliths (FMs) of Si_3N_4/BN (≈85 vol.% Si_3N_4/15 vol.% BN) with three different cell architectures (unidirectional, 0°/90°, and ±45°) were tested in four-point-bend mode under ambient conditions. The FM constituents (hot-pressed monolithic Si_3N_4 and BN) were also characterized. The unidirectional Si_3N_4/BN FM demonstrated the best properties, with ultimate strength of 476 ± 30 MPa and work-of-fracture of 12.6 ± 1.9 kJ/m^2, while Si_3N_4/BN FM with ±45°cell architecture had the lowest strength (175 ± 13 MPa) and work-of-fracture (2.7 ± 1.7 kJ/m^2). The 0°/90° FM had intermediate values of 379 ± 86 MPa and 4.9 ± 2.2 kJ/m^2. High work-of-fracture for the unidirectional Si_3N_4/BN was correlated to toughening mechanisms such as extensive delamination and crack deflection. Predictions for the elastic moduli of the Si_3N_4/BN FMs based on laminate theory correlated well with the observed elastic moduli for the unidirectional and 0°/90° Si_3N_4/BN FMs. However, large discrepancies were observed between predictions and observed values for the ±45° Si_3N_4/BN FMs, possibly due to the increasing role of the BN phase on mechanical properties in these FMs. Mechanical properties of monolithic Si_3N_4 and BN compared well with literature values.

INTRODUCTION

Fibrous monolithic (FM) ceramics, which generally consist of a strong ceramic cell surrounded by a weaker cell boundary, exhibit graceful failure in flexure [1-5]. Fibrous monoliths are produced from powders by conventional ceramic fabrication techniques such as extrusion [1,2]. Several compositions of ceramics and cermets have been processed successfully in fibrous monolithic form [4]. The most thoroughly investigated fibrous monolith consists of Si_3N_4 cells and a continuous BN cell boundary [3-5]. Through appropriate selection of initial powders and extrusion and hot-pressing parameters, tough final products are produced. The high toughness is due primarily to the presence of textured platelike BN grains.

Because of the relatively complex microstructure of FMs, predictive modeling of FM mechanical behavior is not trivial. In this regard, a program has been initiated at Argonne National Laboratory, in collaboration with the University of California, Santa Barbara, to conduct mechanical evaluation and modeling of FM response under mechanical loading.

We report here preliminary results of Si_3N_4/BN fibrous monolithic specimens tested in four-point-bend flexure under ambient conditions. Samples with various cell orientations to the loading direction, including unidirectional, 0°/90°, and ±45°, have been tested. Mechanical properties such as elastic moduli, ultimate strength, and work-of-fracture were measured and the results compared with existing models.

EXPERIMENTAL DETAILS

Fabrication Procedures

The fibrous monoliths were fabricated at Advanced Ceramic Research (ACR), located in Tucson, AZ. They were made from Si_3N_4/BN coextruded green filaments [2] that were 320-330 μm in diameter, flexible, and produced by melt coextrusion of a blend of ≈52 vol.% ceramic powder mixture in an ethylene-based copolymer binder [6]. The coextruded filaments contained nominally 85 vol.% core Si_3N_4 material (E-10, Ube Industries, Tokyo) and 15 vol.% BN cladding (HCP Grade, Advanced Ceramics Corporation, Cleveland). The Si_3N_4 was a sinterable composition, 92 wt.% commercial Si_3N_4 powder, 6 wt.% Y_2O_3, and 2 wt.% Al_2O_3.

Sheets of uniaxially aligned green filaments were produced by a winding operation that placed the coextruded filaments side-by-side on a cylindrical mandrel. The filaments were held in place with a spray adhesive that, upon drying, allowed the unidirectional sheets of green fibrous monolith to be removed from the mandrel. The sheets were then stacked to fabricate the specimens [5]; three laminated architectures were fabricated: 0°, 0/90°, and ±45°. The laminates were cut into the desired preforms and warm-pressed at 160°C to produce a solid green panel.

In this study, simple rectangular flat panels (15.2 x 15. 2 x 0.3 cm) were fabricated for mechanical property evaluation. The panels underwent a binder pyrolysis step that consisted of slow heating in flowing N_2 to 600°C over a period of 42 h. The Si_3N_4/BN panels were then hot-pressed at 1740°C for 1 h under ≈28 MPa pressure. This procedure yielded FM billets with >98% of their theoretical density. Pure BN and Si_3N_4 billets were also hot-pressed.

Nondestructive Evaluations and Microstructural Analysis

The as-received FM plates were examined by thermal imaging for any flaws/inhomogeneites. For microstructural analysis, parallelepiped specimens ≈3 x 3 x 5 mm were cut from the FM and Si_3N_4 billets with a slow-speed diamond-blade saw. All samples were polished to 0.2 μm finish and were examined by scanning electron microscope.

Mechanical Property Evaluations

Monolithic BN and Si_3N_4, and uniaxial, 0°/90°, and ±45° Si_3N_4/BN FM plates were sectioned and tested in flexure under ambient conditions. Typical sample dimensions were ≈3 x 4 x 45 mm. Four-point-bend tests were conducted on samples with inner and outer spans of 15 mm and 40 mm, respectively. For each specimen type, at least three samples were tested. In addition, strain gauges were attached to the tensile surfaces to monitor the stress-strain variation. Thus, strains were measured perpendicular to the hot-pressing direction. The tests were conducted at a constant displacement rate of 1.27 mm/min in an Instron Model 1125 universal tester.

RESULTS AND DISCUSSION

Figure 1 shows thermal images of the as-received Si_3N_4/BN FM plates from ACR with cell orientations of 0°/90° and ±45°. The plates are homogeneous and do not show major flaws or cracks, which is indicative of good processing. However, in the 0°/90° plate, there is some indication of delamination near the top right edge.

Key microstructural features of fibrous-monolithic Si_3N_4/BN are shown in Fig. 2. The cells of the fibrous monoliths were slightly distorted by hot-pressing. Most cells were approximately hexagonal; the maximum cross-sectional dimension was ≈100-200 μm. The BN boundary layer was thin and nearly continuous.

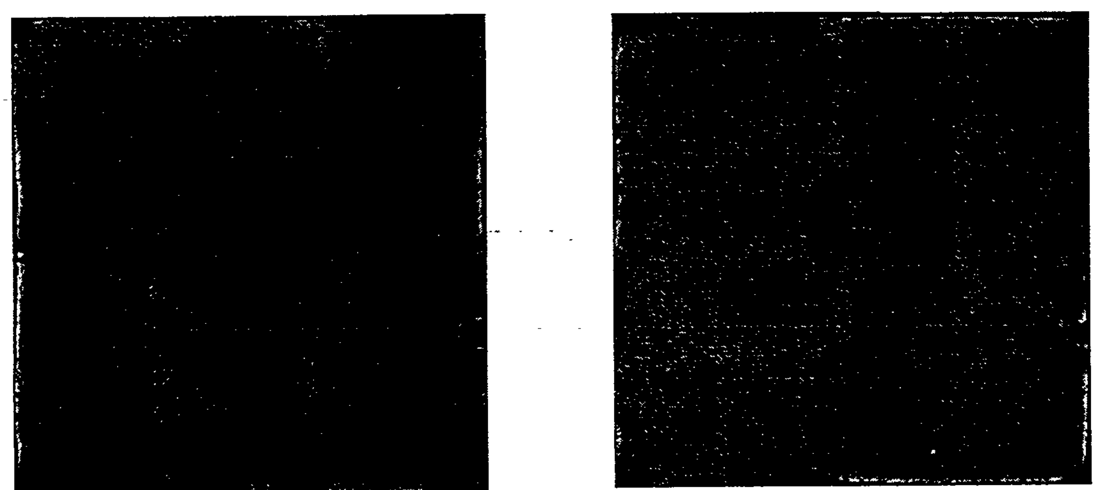

(A) (B)

Fig. 1. Thermal Imaging of As-Received Si_3N_4/BN Fibrous Monolith Plates: (A) 0°/90° and (B) ±45° Cell Orientations

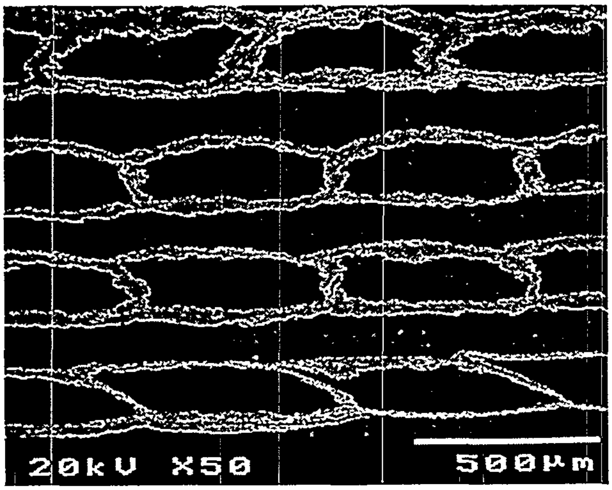

Fig. 2. Microstructure of 0°/90° Si_3N_4/BN Fibrous Monolith

Typical load-displacement plots for monolithic Si_3N_4, and Si_3N_4/BN FMs samples are shown in Fig. 3. The load increases linearly and is followed by a precipitous drop. After the peak load, load-carrying ability of all FMs was significantly superior to that of monolithic Si_3N_4. Moreover, the peak loads obtained were highest for the uniaxial samples and lowest for the ±45° oriented FMs. Average strength values, determined from the peak loads, for the various samples tested are given in Table 1. Work-of-fracture of the FMs was determined from the area under the load-displacement plots.

Typical linear stress-strain variations obtained for BN, Si_3N_4, and Si_3N_4/BN FMs are shown in Fig. 4. For all samples tested, failure strains ranged from 1000-2000 με. For ±45° Si_3N_4/BN FMs, significant deviation from linearity was observed. Elastic moduli for the various ceramics were determined from the slope of linear region of stress-strain plots (see Table 1).

The stress-strain variations of BN deviate from linearity at higher stresses. This may be a result of slippage/microcrcaking along the BN layers [4]. The elastic modulus of 20.7 GPa for BN is in excellent agreement with the value of 19-23 GPa reported in the literature [7]. As expected, monolithic Si_3N_4 shows a linear stress-strain behavior. The elastic modulus determined for monolithic silicon nitride is in reasonable agreement with typical reported literature values of 250-300 GPa [8].

The results show that the strength and Young's modulus values for FM samples are lower than those of monolithic silicon nitride. However, the FMs display significant ability to sustain loads after the first cracking, as shown by their high work-of-fracture values. Flexural strength, Young's modulus, and work-of-fracture are highest for the uniaxial architecture, followed by the 0°/90° architecture, and are lowest for the ±45° architecture.

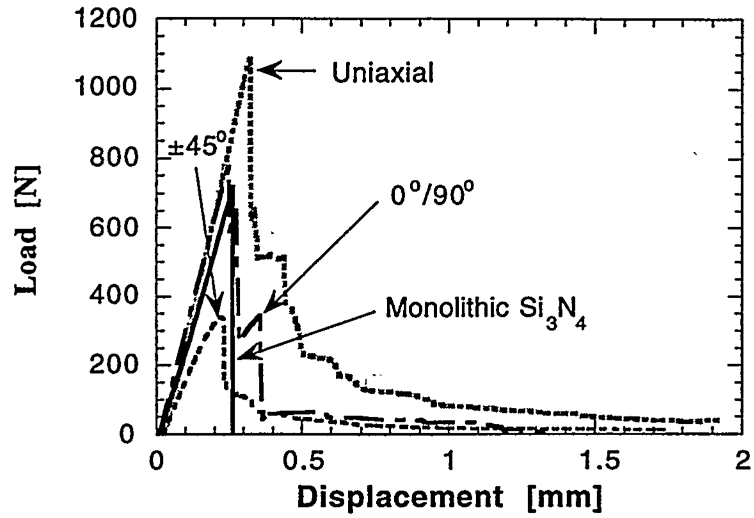

Fig. 3. Typical Load-Displacement Variations of Si_3N_4/BN Fibrous Monoliths and Monolithic Si_3N_4 Tested in a Four-Point-Bend Mode

Laminate theory was used to predict Young's moduli for the investigated architectures. For the uniaxial architecture, the well-known Voight rule-of-mixtures was used:

$$E_l = E_{BN}V_{BN} + E_{SN}(1 - V_{BN}),$$

where E_{BN} and E_{SN} are the Young's moduli of boron nitride and silicon nitride, respectively, obtained in mechanical testing of monolithic specimens of boron nitride and silicon nitride, and V_{BN} is the volume fraction of the boron nitride phase and was taken to be 0.15. For the multiaxial architectures, the Young's moduli are calculated on the basis of the results for the unidirectional FMs as per laminate theory [9]. The Young's modulus values match well with the predictions from laminate theory for uniaxial and 0°/90° architecture; however, there is a large discrepancy between the predicted and measured values of the Young's modulus for the ±45° architecture. This may be due to the increased role of the weak BN phase in stress distribution in specimens with such fibroid orientation.

Table 1. Mechanical Properties of Si_3N_4 and Si_3N_4/BN FMs

Sample	Measured Young's Modulus (GPa)	Predicted Young's Modulus (GPa)	Flexural Strength (MPa)	Work-of-Fracture (kJ/m^2)
Si_3N_4	242 ± 5	-	677 ± 127	-
BN	21	-	38 ± 3	-
Si_3N_4/BN (uniaxial)	216 ± 2	209	476 ± 30	12.6 ± 1.9
Si_3N_4/BN (0°/90°)	158 ± 34	167	379 ± 86	4.9 ± 2.2
Si_3N_4/BN (±45°)	92 ± 15	150	175 ± 13	2.7 ± 1.7

Measured work-of-fracture values for the three Si_3N_4/BN FM sets range from 12.6 kJ/m^2 for unidirectional FMs to as low as 2.7 kJ/m^2 for ±45° FMs. These values are comparable to some of the continuous fiber-reinforced ceramic matrix composites. The dependence of work-of-fracture on fibroid orientation in FMs is related qualitatively to the failure modes. As shown in Fig. 5, failure in unidirectional FMs was associated with toughening mechanisms such as extensive delamination and crack deflection. This propensity for delamination and crack deflection reduced considerably in the multidirectional FMs with 0°/90° and ±45° orientations, as evidenced in their failure modes (Fig. 6 and 7).

SUMMARY

1. Mechanical properties of monolithic Si_3N_4, BN, and Si_3N_4/BN with three different orientations (unidirectional, 0°/90°, and ±45°) were evaluated under ambient conditions.
2. Mechanical property data for monolithic Si_3N_4 and BN were similar to those reported in the literature.
3. Si_3N_4/BN FMs with unidirectionally oriented architecture showed superior mechanical properties (moduli, ultimate strength, and work-of-fracture) relative to those of Si_3N_4/BN FMs with 0°/90° and ±45° architectures.
4. Measured Young's moduli for unidirectional and 0°/90° Si_3N_4/BN FMs correlated well with the theoretical predictions based on laminate theory. However, for ±45° Si_3N_4/BN FM, the predictions were significantly higher than the observed values. This discrepancy is believed to be due to the increased role of the BN phase in failure of these FMs.
5. Work-of-fracture for the Si_3N_4/BN FMs was correlated to their modes of fracture.

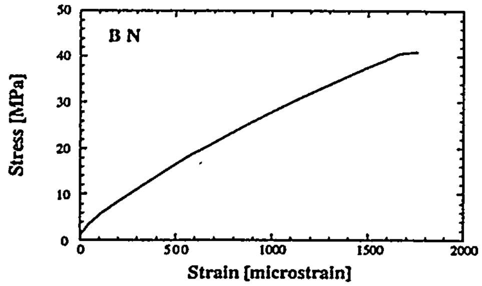

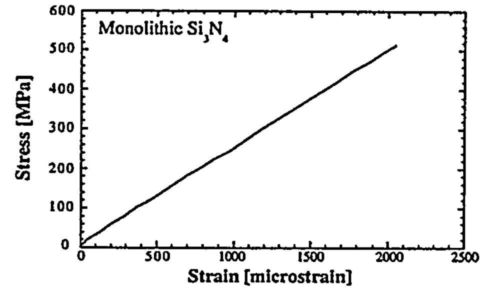

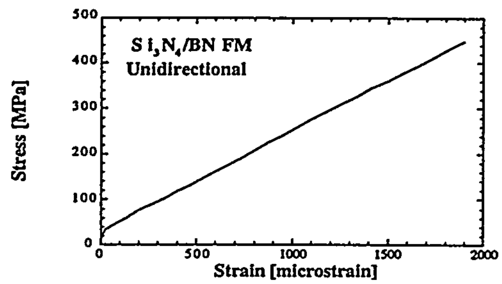

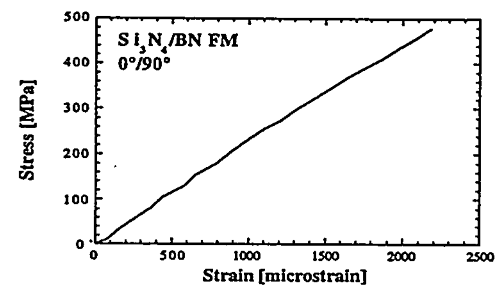

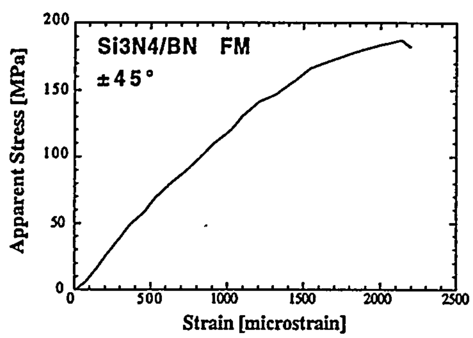

Fig. 4. Stress-Strain Behavior of BN, Si_3N_4 and Si_3N_4/BN Fibrous Monoliths with Various Cell Orientations: 0°, 0°/90°, and ±45°

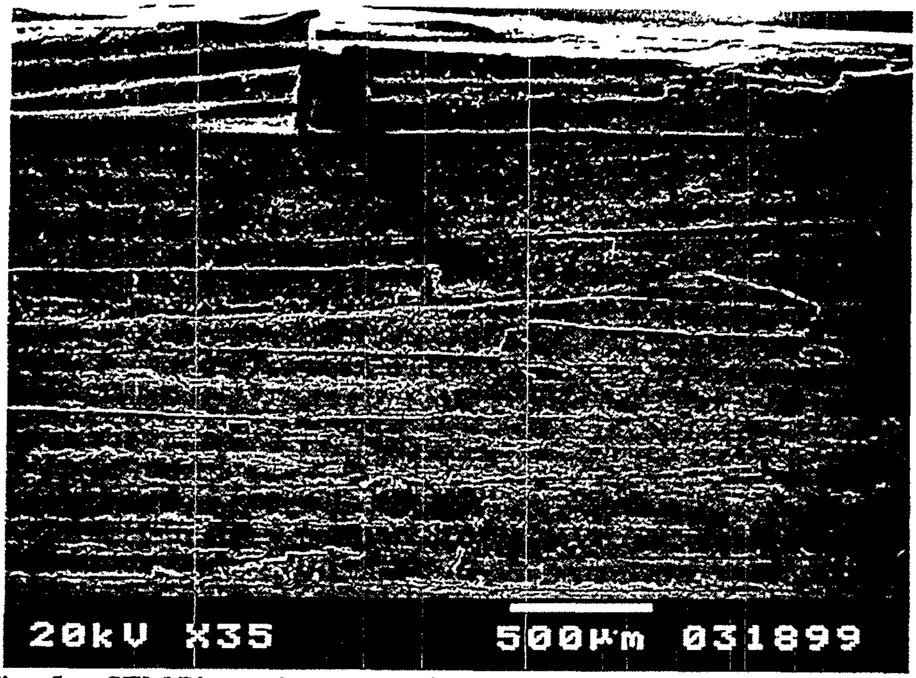

Fig. 5. SEM Photomicrograph of Fractured Unidirectional Si_3N_4/BN FM Showing Extensive Delamination and Crack Deflection

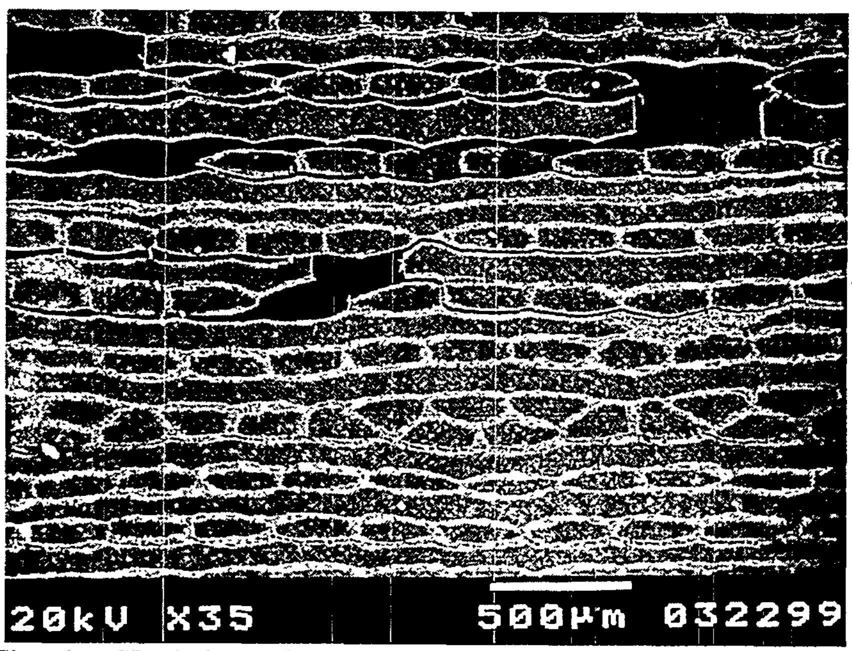

Fig. 6. SEM Photomicrograph of Fractured 0°/90° Si_3N_4/BN FM Showing Limited Delamination and Crack Deflection

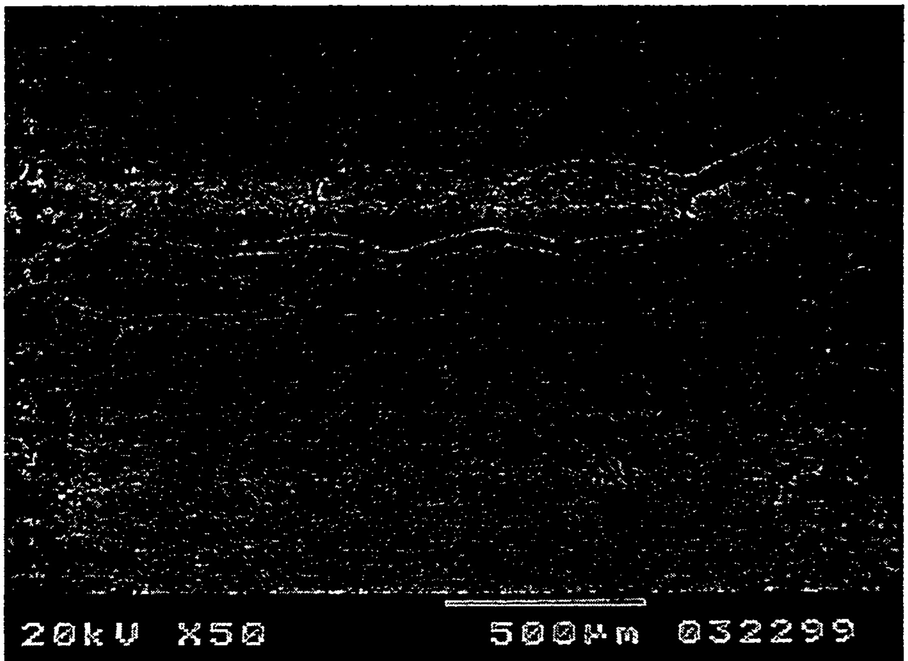

Fig. 7. SEM Photomicrograph of Fractured ±45° Oriented Si_3N_4/BN FM Showing Limited Delamination and Crack Deflection

ACKNOWLEDGMENTS

This work was supported by the Defense Advanced Research Projects Agency through a U.S. Department of Energy Interagency Agreement, under Contract W-31-109-Eng-38 at Argonne National Laboratory.

REFERENCES

1. W. S. Coblenz, "Fibrous Monolithic Ceramic and Method for Production," U.S. Patent 4,772,524, Sept. 20, 1988.
2. D. Popovic, J. W. Halloran, G. E. Hilmas, G. A. Brady, S. Somas, A. Bard, and G. Zywicki, "Process for Preparing Textured Ceramic Composites," U.S. Patent 5,645,781, July 8, 1997.
3. G. Hilmas, G. A. Brady, U. Abdali, G. Zywicki, and J. Halloran, "Fibrous Monoliths: Non-brittle Fracture from Powder-processed Ceramics," Mater. Sci. Eng. **A195**, 263-68 (1995).
4. D. Kovar, B. H. King, R. W. Trice, and J. W. Halloran, "Fibrous Monolithic Ceramics," J. Am. Ceram. Soc. **80**, 2471-87 (1997).
5. G. A. Danko, G. E. Hilmas, J. W. Halloran, and B. King, "Fabrication and Properties of Quasi-isotropic Silicon Nitride-Boron Nitride Fibrous Monoliths," Ceram. Eng. Sci. Proc. **18** [3], 607-13 (1997).
6. G. A. Brady, G. E. Hilmas, and J. W. Halloran, "Forming Textured Ceramics by Multiple Coextrusion," pp. 609-614 in *Ceramic Transactions, Vol. 51,*

Ceramic Processing Science and Technology. Eds. H. Hausner and G. Messing. American Ceramic Society, Westerville, OH, 1995.

7. J. H. Edgar, "Crystal Structure, Mechanical Properties and Thermal Properties of BN," pp. 7-21 in Properties of Group III Nitrides, Ed. J. H. Edgar, INSPEC, London, U.K. (1994).
8. M. L. Torti, "The Silicon Nitride and Sialon Families of Structural Ceramics", in Treatise of Materials Science and Technology, Ed. J. H. Wachtman, Vol. 29, Academic Press New York (1989).
9. M. Daniel and O. Ishai, *Engineering Mechanics of Composite Materials;* pp. 48-183. Oxford University Press, Oxford, U.K., 1994.